DOI:
10.1080/00207721.2019.1654006

Document Version
Peer reviewed version

Citation for published version (APA):
Wen, S., Zhang, D., Zhang, B., Lam, H. K., Wang, H., & Zhao, Y. (2019). Two-degree-of-freedom internal model position control and fuzzy fractional force control of nonlinear parallel robot. *INTERNATIONAL JOURNAL OF SYSTEMS SCIENCE*, *50*(12), 2261-2279. https://doi.org/10.1080/00207721.2019.1654006

Two-Degree-of-Freedom Internal Model Position Control and Fuzzy Fractional Force control of nonlinear Parallel Robot

Shuhuan Wen[1*], Di Zhang[1], Baowei Zhang[1], Hak Keung Lam[2] ,Hongbin Wang[1] and Yongsheng Zhao[3]

[1]*Key Lab of Industrial Computer Control Engineering of Hebei Province, Yanshan University, Qinhuangdao, 066004,China*

[2]*Department of Informatics, Kings College London, Strand, London, WC2R 2LS, United Kingdom;*

[3]*Parallel Robot and Mechatronic System Laboratory of Hebei Province and Key Laboratory of Advanced Forging &Stamping Technology and Science of Ministry of National Education, Yanshan University, Qinhuangdao, 066004, China*

Email: swen@ysu.edu.cn, 1120067126@qq.com, 458110801@qq.com,

hak-keung.lam@kcl.ac.uk, hb_wang@ysu.edu.cn, yszhao@ysu.edu.cn

ABSTRACT

The paper proposes a novel method for the nonlinear redundantly actuated parallel robot based on force/position hybrid control structure. In order to solve the limitation of making a compromise for internal model controller, a two-DOF fractional order internal model control algorithm combining the internal model control principle and the fractional order theory is proposed for the position branch of the parallel robot redundantly actuated. This algorithm can realize the adjustment of the dynamic performance and anti-interference of 6PUS-UPU respectively. Aiming at the big force control error fractional order internal model, fuzzy control theory and the fractional order internal model controller are integrated into a new controller-fuzzy fractional order internal model(FFOIM) force control algorithm. Then Admas/Matlab simulation results demonstrate that the proposed algorithm can further reduce the driving force error of the system, and also retain the strong anti-interference of fractional order internal model controller.

KEYWORDS

Parallel robot, Force/position hybrid control, Fuzzy Fractional order, Internal model control

1. Introduction

Parallel robot plays an important role in the manufacturing, logistics and even military fields because of its large stiffness, high carrying capacity, good dynamic performance. At present, the control methods of redundant parallel robot still need to learn from the latest technology of non-redundant parallel robot and even series robot, and do further research for the control methods of redundant parallel robot(Krzysztof Tchoń et al.,2016;Wen H et al., 2015;Sébastien B. et al., 2017;Pham Q C et al., 2015;Taghirad H D et al., 2011). The 6PUS/UPU redundantly actuated parallel robot studied in this paper has complex structure and high control precision requirement. The superiority of the control performance is directly related whether the parallel robot can satisfy the high speed and high precision requirement. In this paper, the force/location hybrid control structure is used. The first five branches are position control mode, which can determine the motion precision of the moving platform. The sixth branch uses the torque control mode, which can optimize the driving force and improve the overall performance of the 6PUS-UPU.

In order to solve the control precision problem of redundant actuation parallel robot, many scholars have applied advanced intelligent control theory to high performance system. The internal model control algorithm(IMC) can effectively improve the motion error precision and enhance the anti-interference of control system, which has been widely concerned by many scholars. In Savran A I, Beke A, Kumbasar T, et al.(2015), a simple and self-adjusting IMC-API controller was proposed for small industrial water tank. The experimental result showed that the proposed method can enhance the robustness of the system and restrain the parameter disturbance. In Wang Z et al.(2016), the authors designed a kind of double internal model controller for hydraulic quadruped robot joint force control. And the results showed that it further improved the system accuracy. The work in (Kostić M D et al., 2016) applied the modified internal model method to rehabilitation robot. The experiment results indicated that the proposed method did well in positional error between the target and the reached position. Wen S et al.(2016) introduced the model predictive control (MPC) algorithm into the torque control of the redundant branch, which improves the control precision of the driving force of the parallel robot. But the position branches of the 6PUS-UPU redundantly actuated parallel robot used the PID control method. The control precision of the robot is not greatly promoted.

In the area of industrial control, the application of conventional IMC is limited in the complex characteristics process such as nonlinearity(Hou Y et al., 2016), time-varying parameters(Pagavathigounder B et al., 2016) and uncertainty. It is difficult to obtain satisfied control effect. Internal model controller can be combined with other control methods in order to obtain a new method with the advantages of two kinds of control methods at the same time. Fractional order internal model controller(FOIMC) combines the advantages of internal model controller and fractional order controller. Only one parameter need to be adjusted, which can be regarded as a new controller design idea.

In Sondhi S and Hote Y V(2014), a fractional order internal model controller is proposed for the fractional-order gas turbine system. This controller has a smaller error compared with other forms of internal model controller. In Li D, Fan W, Jin Q, et al.(2010), a fractional order IMC-PID controller is designed based on the fractional order system. The simulation results show that the method has a smaller error compared with the integer order IMC method. In Maâmar B and Rachid M(2014), the controller based on IMC-PID Fractional order filter is proposed for integer-order controlled object. The controller is validated on the first-order time-delay model. The simulation results show that it has good tracking performance and anti-interference performance.

Although fractional order internal model controller possesses superior performance, it is a one-DOF controller. It often need to make a compromise between the tracking performance and anti-interference performance. One-DOF internal controller has some limitations for the redundant actuation parallel robot with high precision requirement, so it is difficult to obtain better control effect.

Many scholars have combined advanced algorithms with the internal model control in order to better solve high standard control requirements for high-performance systems. In Zhu Q et al.(2016), a two-DOF internal model controller was designed for the motor drive system, which can improve motion precision and anti-interference capability of the system. The method includes two adjustable parameters, which can affect dynamic performance and robust performance of the system respectively. In Liu X et al.(2014), a two-DOF controller was designed for electric pitch servo system. The controller is composed of two adjustable parameters, which can realize to adjust the trajectory tracking performance and anti-interference performance of the accurate position platform respectively. The Vinopraba T et al.(2011) proposed a two-DOF internal model controller based on fractional order theory, which improved the compromise between the anti-interference and the tracking performance for one-DOF internal model controller.

The redundant branches of the parallel robot can effectively solve the problems of small workspace and singular configuration. However, the redundant actuation can cause strong coupling effect among each branch of the parallel robot, which makes the control system very complex. The traditional AC servo system usually uses conventional PID control strategy, but PID is difficult to meet high control precision requirement for the parallel robot. Fuzzy control strategy doesn't need the mathematical model of the controlled object, and has good robustness(Lakshmana G N V et al., 2016). It is suitable for time-varying and nonlinear systems(Zhong Z et al., 2016). So fuzzy control strategy is combined with PID and fractional order theory, a new research area will appear. In order to further to improve the trajectory tracking, a fractional order fuzzy-PID controller is proposed in Reham, H et al.(2016). The results showed in all discussed cases that the results of fractional fuzzy-PID controller is better than the results of FOPID and fuzzy-PID controller. The authors in Delavari H et al.(2010)applied fuzzy fractional order sliding mode controller to nonlinear systems, the simulation results signify performance of genetic-based fuzzy fractional sliding mode controller. A novel fractional order fuzzy control method for a class of fractional order non-linear systems is proposed in Wang B et al.(2016). The proposed control scheme is developed for fractional order nonlinear systems stabilization under random disturbances. Simulation results demonstrated the designed fractional order T-S fuzzy control scheme works well compared with the existing other methods. Wen S et al.(2017) obtained the fuzzy T-S model of the 6PUS-UPU redundantly actuated parallel robot dynamic model by the fuzzy identification method. And in order to solve the force delay problem of redundant driving force branch, the authors designed the Smith predictor compensator to solve the delay problem. The simulation results show that the proposed method can obtain the ideal fuzzy T-S model and eliminate the delay problem of the force branch. However the position branches of the parallel robot PID control method, which cannot guarantee the accuracy of the parallel robot movement. The force branch used the PI control method, however it cannot improve the anti-interference performance of the robot. Because parallel robot is widely used in high-performance and high-precision applications, we need not only to improve the position precision of the robot, but also to reduce the internal forces to improve the overall performance of the robot.

This paper has the following contributions. In order to solve the limitation of making a compromise for internal model controller, a two-DOF fractional order internal model control algorithm combining the internal model control principle and the fractional order theory is proposed for the position branch of the redundant actuation parallel robot. This algorithm can realize the adjustment of the dynamic performance and anti-interference of 6PUS-UPU respectively. Aiming at the big force control error for fractional order internal model, fuzzy control theory and the fractional order internal model controller are integrated into a new controller-fuzzy fractional order internal model(FFOIM) force control algorithm because fuzzy control is easy to implement, has good robustness and doesn't need the mathematical model of the controlled object. Then the joint simulation demonstrates that the proposed algorithm can further reduce the driving force error of the system, and also retain the strong anti-interference of fractional order internal model controller. In contrast with previous work (Wen S et al., 2017; Wen S et al., 2016), the algorithms proposed by this paper not only possess high tracking performance and can adjust the tracking performance and anti-interference performance according to requirements, but also guarantee the driving force control precision of the system and optimize the internal force of the system.

The remainder of the paper is organized as follows. In section 2, the model of the 6PUS-UPU redundantly actuated parallel robot is introduced, and the driving force is optimized by KANE method. The two-DOF fractional order internal model position control and fuzzy internal model fractional order force control of the robot are detailed in section 3. The results of the joint simulation are discussed in section 4. Concluding remarks are given in section 5.

2. The dynamics model

This section mainly introduces the structure characteristics of 6PUS-UPU redundantly actuated parallel robot. 6PUS-UPU redundantly actuated parallel robot consists of moving platform, fixed platform, six actuators which connect the moving platform and fixed platform, and a constraint branch. The six actuators connect the moving platform and fixed platform through prismatic pair (p), universal joint (u), and spherical hinge (s). The constraint branch connects the two platforms through two universal joints (u). Fig.1 shows the structure of 6PUS-UPU redundantly actuated parallel robot. The velocity, the acceleration, the partial velocity, the partial acceleration of 6PUS-UPU are introduced in (Wen S et al., 2017;Wen S et al., 2016), and driving force of each branch is obtained. Based on our previous work in the Wen S et al.(2017) and Wen S et al.(2016), the generalized driving force $\boldsymbol{F}_j^{\,r}$ and the generalized inertia force $\boldsymbol{F}_j^{\,*r}$ of the parallel robot are obtained. According to KANE equation, we can get the dynamics equation of the 6PUS-UPU redundantly actuated parallel robot. The driving force of the six branches, the binding force and the constraint torque of the constraint branch in dynamics equation are separated, we can get

$$\boldsymbol{F}_j^{\,r} + \boldsymbol{F}_j^{\,*r} = \boldsymbol{G}\left[\boldsymbol{F}_{q1}\,\boldsymbol{F}_{q2}\,\boldsymbol{F}_{q3}\,\boldsymbol{F}_{q4}\,\boldsymbol{F}_{q5}\,\boldsymbol{F}_{q6}\,\boldsymbol{M}_c\right] - \boldsymbol{F}'^{T} = 0 \tag{1}$$

$$\boldsymbol{G\tau} = \boldsymbol{F}'^{\mathrm{T}} \tag{2}$$

$$\boldsymbol{G} = \begin{bmatrix} \boldsymbol{n}_1 & \boldsymbol{n}_2 & \boldsymbol{n}_3 & \boldsymbol{n}_4 & \boldsymbol{n}_5 & \boldsymbol{n}_6 & \boldsymbol{0} \\ \boldsymbol{r}_1 \times \boldsymbol{n}_1 & \boldsymbol{r}_2 \times \boldsymbol{n}_2 & \boldsymbol{r}_3 \times \boldsymbol{n}_3 & \boldsymbol{r}_4 \times \boldsymbol{n}_4 & \boldsymbol{r}_5 \times \boldsymbol{n}_5 & \boldsymbol{r}_6 \times \boldsymbol{n}_6 & \boldsymbol{s} \end{bmatrix}$$

where $\boldsymbol{G}$ is the Jacobian matrix of the parallel robot under redundancy, τ is the optimized driving force, $\boldsymbol{F}'^{T}$ is the load acted on the moving platform.

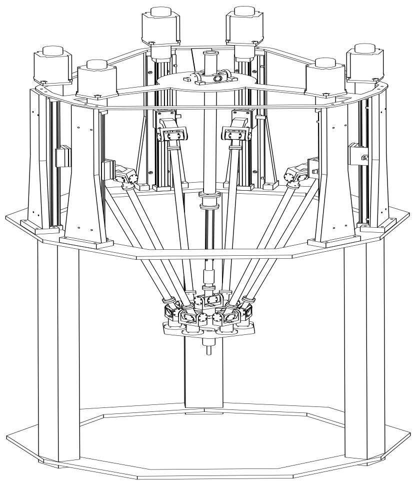

Figure 1. The structure of 6PUS-UPU redundantly actuated parallel robot

The redundant actuation parallel robot in this paper has five degrees of freedom, but it has six inputs. It means that even if the output force of the moving platform is given, it is impossible to determine the only driving input torque. This directly causes that one output situation corresponds to an infinite input, so it is difficult to do quantitative analysis for the input and output of the mechanism. So the driving force need to be optimized.

The optimization methods of the driving force mainly include force optimization and energy consumption optimization. Energy consumption optimization method can effectively improve system efficiency, but could cause the problem that excessive driving force fluctuation of the mechanism appears. In this paper, the main purpose of driving force optimization of the 6PUS-UPU parallel robot is to balance the internal force of the parallel mechanism, and improve the motion precision of the moving platform. So in this paper, the two-norm minimization method is used to optimize the driving force of the mechanism (Wen S et al., 2017;Wen S et al., 2016).

The two-norm minimization method is:

$$\begin{cases} \min\ \boldsymbol{Z} = \boldsymbol{\tau}^{\mathrm{T}} \boldsymbol{W} \boldsymbol{\tau} \\ s.t.\ \boldsymbol{G}\boldsymbol{\tau} = \boldsymbol{F}'^{\mathrm{T}} \end{cases} \tag{3}$$

In order to solve the optimized redundant driving force $\boldsymbol{\tau}$, the optimization problem of the driving force is transformed into solving the conditional extreme value by introducing the Lagrange factor $\boldsymbol{\lambda}$:

$$\boldsymbol{Z}' = \boldsymbol{\tau}^{\mathrm{T}} \boldsymbol{W} \boldsymbol{\tau} + \boldsymbol{\lambda}^{\mathrm{T}} \left(\boldsymbol{F}'^{\mathrm{T}} - \boldsymbol{G}\boldsymbol{\tau} \right) \tag{4}$$

In order to obtain the minimum value of $\boldsymbol{Z}'$, the Eq.(4) need satisfy the following conditions.

$$\frac{\partial \boldsymbol{Z}'}{\partial \boldsymbol{\tau}} = 2\boldsymbol{\tau}^{\mathrm{T}} \boldsymbol{W} - \boldsymbol{\lambda}^{\mathrm{T}} \boldsymbol{G} = 0 \tag{5}$$

$$\frac{\partial \boldsymbol{Z}'}{\partial \boldsymbol{\lambda}} = \boldsymbol{F}'^{\mathrm{T}} - \boldsymbol{G}\boldsymbol{\tau} = 0 \tag{6}$$

According to Eq.(5), we can get the equation as follows.

$$\boldsymbol{\tau} = \frac{1}{2} \left(\boldsymbol{W}^{-1} \right)^{\mathrm{T}} \boldsymbol{G}^{\mathrm{T}} \boldsymbol{\lambda} \tag{7}$$

Substitute Eq.(7) into Eq.(6).

$$\boldsymbol{\lambda} = 2(\boldsymbol{G}(\boldsymbol{W}^{-1})^{\mathrm{T}} \boldsymbol{G}^{\mathrm{T}})^{-1} \boldsymbol{F}' \tag{8}$$

Substitute Eq.(8) into Eq.(5).

$$\boldsymbol{\tau} = \left(\boldsymbol{W}^{-1} \right) \boldsymbol{G}^{\mathrm{T}} \left(\boldsymbol{G} \left(\boldsymbol{W}^{-1} \right) \boldsymbol{G}^{\mathrm{T}} \right)^{-1} \boldsymbol{F}'^{\mathrm{T}} \tag{9}$$

If $\boldsymbol{W}$ is the unit matrix, the optimal solution of the driving force is

$$\begin{aligned}\boldsymbol{\tau} &= \boldsymbol{G}^{\mathrm{T}}\left(\boldsymbol{G}\boldsymbol{G}^{\mathrm{T}}\right)^{-1}\boldsymbol{F}'^{\mathrm{T}} \\ &= \boldsymbol{G}^{+}\boldsymbol{F}'^{\mathrm{T}}\end{aligned} \tag{10}$$

Where $\boldsymbol{G}$ is the irreversible matrix, $\boldsymbol{G}^{+}$ is the pseudo inverse of $\boldsymbol{G}$.

3 The design of the controller

The control strategy is the most important tropic for parallel robot, and the reasonable and practical control strategy should be used to exert the high performance of parallel robot. In Wen S et al.(2017) and Wen S et al.(2016), a force/position hybrid control strategy is proposed. The first five branches of the parallel mechanism use the position control strategy to ensure the position precision of moving platform of the parallel robot. The redundant branch uses the torque control strategy to optimize internal force of the parallel mechanism, which can improve the overall performance of the 6PUS-UPU parallel robot.

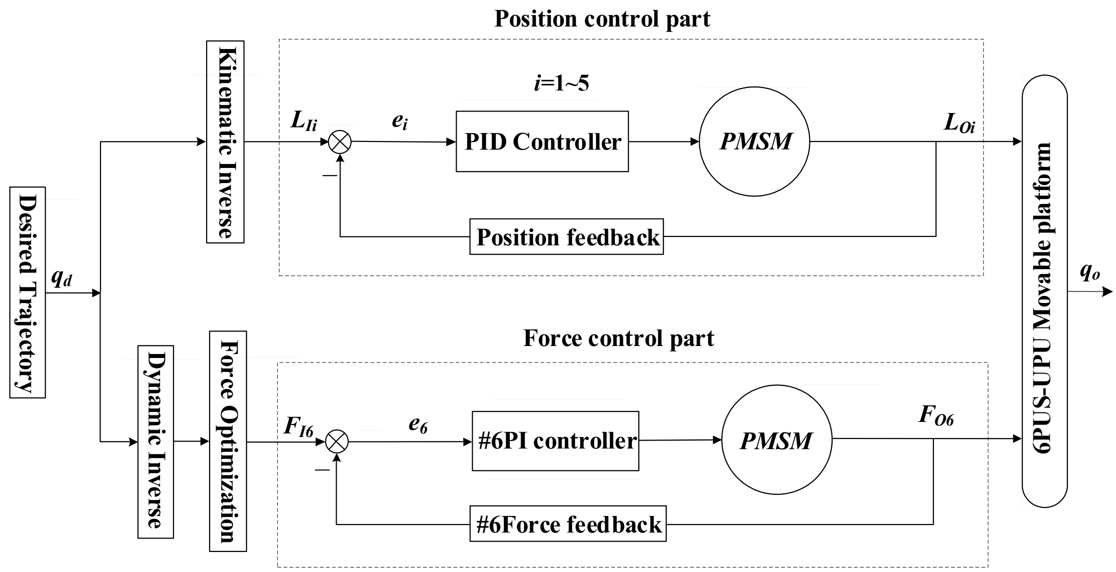

Figure 2. The force/position hybrid control diagram of the 6PUS-UPU redundant actuation parallel robot

Then the controllers of the position branches and the force branch are designed respectively. Figure 2 shows the structure of the force/position hybrid control strategy of each branch of the redundantly actuated parallel robot.

3.1 The internal model position controller of the two-DOF fractional order

The vector control method can improve the AC servo system performance, and make that the AC servo system has good DC motor performance. So the application of AC servo system is widely used in the industrial robots. Because the structure of the AC servo system is simple and easy to implement, the three-closed-loop control method is used. Figure 3 is the three-closed-loop control method diagram.

In Figure 3, G_{APR}, G_{ASR} and G_{ACR} represent the position loop regulator, the speed loop regulator and the current loop regulator respectively.

However, there exist time-varying parameters, load disturbances and uncertain factors in AC servo systems. Conventional three-closed-loop control is difficult to meet the requirement of the system with good tracking performance and anti-interference performance at the same time. So the satisfied control effect is often difficult to obtain for the high performance control system. Fractional order internal model(FOIM) is an advanced control strategy with the advantages of convenient parameters adjustment and strong robustness. In this paper, a fractional-order internal model control algorithm is proposed to improve the precision and the robustness of the position branches.

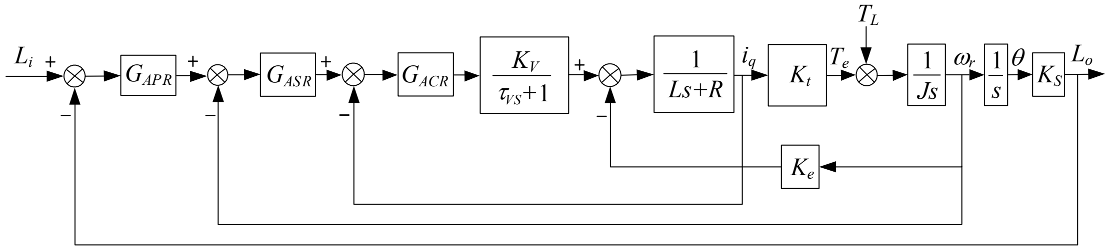

Figure 3. Three-closed-loop control block diagram

The internal model control diagram is shown in Figure 3.

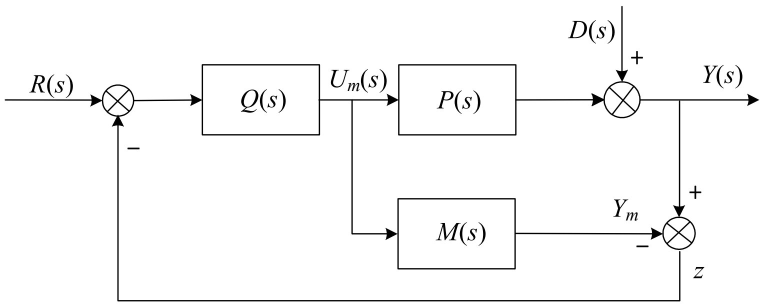

Figure 4. Internal model control diagram

In Figure 4, $Q(s)$, $P(s)$ and $M(s)$ represent the internal model controller, the controlled object and the object model respectively, $R(s)$, $Y(s)$ and $D(s)$ represent the input, the output and the interference signal of the system respectively.

According to Figure 4, the input/output relationship can be obtained as follows.

$$\begin{cases} \dfrac{Y(s)}{R(s)} = \dfrac{Q(s)P(s)}{1+Q(s)[P(s)-M(s)]} \\ \dfrac{Y(s)}{D(s)} = \dfrac{1-Q(s)M(s)}{1+Q(s)[P(s)-M(s)]} \end{cases} \tag{11}$$

Then the closed-loop response in Figure 4 can be obtained.

$$Y(s) = \frac{Q(s)P(s)R(s)}{1+Q(s)[P(s)-M(s)]} + \frac{1-Q(s)M(s)}{1+Q(s)[P(s)-M(s)]} D(s) \tag{12}$$

When the model is accurate, that is, $P(s) = M(s)$, as long as $Q(s)$ and $M(s)$ is stable, then the internal model controller achieves stable closed-loop control. In this case, if the inverse of the minimum phase of the system model $M(s)$ exists, and the internal model controller $Q(s) = M(s)$, then the system is in the ideal control state, that is, $Y(s) = R(s)$. In practical situation, the internal model controller needs to connect a low-pass filter $f(s)$ in series. It not only can ensure $Q(s)$ to be implemented easily, but also can adjust the performance of the system. The internal model controller has the following form.

$$Q(s) = M_{-}^{-1}(s) f(s) \tag{13}$$

Where $M_{-}^{-1}(s)$ is the inverse of the minimum phase of the model $M_{-}(s)$. $f(s)$ is a low-pass filter. In order to ensure $Q(s)$ rational, so $f(s)$ is usually selected as:

$$f(s) = \frac{1}{(1 + \lambda s)^r} \tag{14}$$

Where r must be large enough in order to ensure $Q(s)$ reasonable. λ is the time parameter of the filter, which is the only adjustable parameter in the internal model controller. Transform Figure 4 into the traditional feedback control system shown in Figure 5.

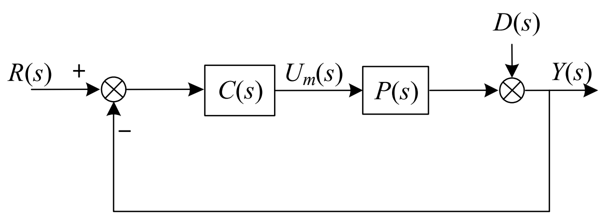

Figure 5. Equivalent traditional feedback control diagram

In Figure 5, $C(s)$ is a designed internal model controller. The relationship among $C(s)$, $Q(s)$ and $M(s)$ is expressed as follows.

$$\begin{cases} C(s) = \dfrac{Q(s)}{1 - M(s)Q(s)} \\ Q(s) = \dfrac{C(s)}{1 + M(s)C(s)} \end{cases} \tag{15}$$

In this paper, a fractional order internal model PD controller is designed based on the PMSM model. Considering the system stability and simplicity, the controlled object of the position loop can be equivalent to the I type system, that is, the form of $M(s)$ is as Eq.(16).

$$M(s)=\frac{K}{s(Ts+1)} \tag{16}$$

In order to get the fractional order controller, the low-pass filter is:

$$f(s)=\frac{2\lambda s^{\alpha}+1}{\left(\lambda s^{\alpha}+1\right)^{2}} \tag{17}$$

Then the equivalent feedback controller $C(s)$ is:

$$C(s)=\frac{\left(2\lambda s^{\alpha}+1\right)\left(Ts+1\right)}{K\lambda^{2}s^{2\alpha-1}} \tag{18}$$

$C(s)$ is simplified to a fractional-order PID structure, and in series with the fractional order filter to satisfy the characteristics of the closed-loop fractional order.

$$C(s)=\frac{1}{s^{\alpha-1}}\cdot\left(\frac{2}{K\lambda}+\frac{2T}{K\lambda}s\right)+\frac{1}{s^{2\alpha-1}}\cdot\left(\frac{1}{K\lambda^{2}}+\frac{T}{K\lambda^{2}}s\right) \tag{19}$$

Eq.(19) is the fractional order internal model controller. It is obvious that there are only two adjustable parameters λ and α. The filter order α and the parameter λ affect the overshoot and the settling time of the system respectively. It is convenient to adjust two parameters to obtain good control effect. But the adjustment of parameters requires a trade-off between dynamic performance and robustness. So in this paper a two-DOF fractional order internal model controller is proposed, which can meet the dynamic performance and robustness of the system at the same time.

The diagram of the AC servo position system controlled by the two-DOF internal model controller is shown in Figure 6.

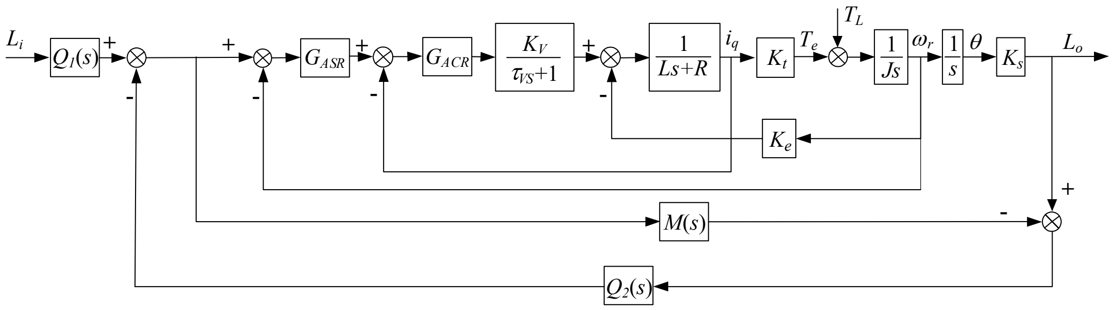

Figure 6. The structure of the two-DOF internal model controller of AC servo system

Figure 6 can be equivalent to Figure 7. In Figure 6 and Figure 7, $C1(s)=\dfrac{Q1(s)}{Q2(s)}$, $C2(s)=\dfrac{Q2(s)}{1-M(s)Q2(s)}$. So $Q1(s)$, $Q2(s)$ can be designed at first, then the design of $C_1(s)$ and $C_2(s)$ can be completed. The position loop of the controlled object is simplified as I type system $M(s)=\dfrac{K}{s(Ts+1)}$.

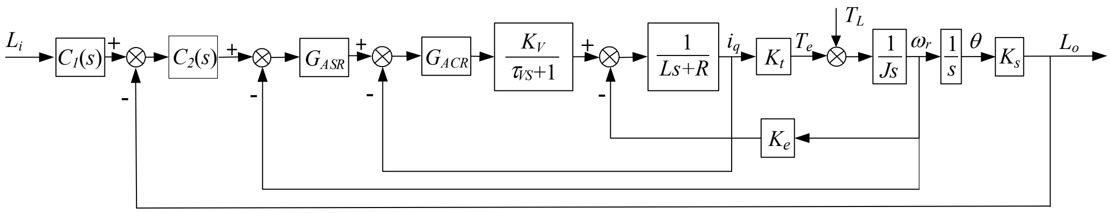

Figure 7. The equivalent structure diagram of the two-DOF internal model control of AC servo system

According to the IMC design principle, $Q_1(s)$ and $Q_2(s)$ can be chosen as follows.

$$\begin{cases} Q_1(s)=f_1(s)\cdot M^{-1}(s) \\ Q_2(s)=f_2(s)\cdot M^{-1}(s) \end{cases} \tag{20}$$

Where $f1(s)$ and $f2(s)$ are low-pass filter.

In order to make the parallel robot obtain good steady-state performance and dynamic performance, and adjust the tracking performance and anti-interference performance of the system respectively, the low-pass filter chosen in the paper is:

$$
\begin{cases}
f_1(s)=\dfrac{2\lambda_1 s^{\alpha_1}+1}{\left(\lambda_2 s^{\alpha_2}+1\right)^2} \\
f_2(s)=\dfrac{2\lambda_2 s^{\alpha_2}+1}{\left(\lambda_2 s^{\alpha_2}+1\right)^2}
\end{cases}
\tag{21}
$$

According to the relationship of $C(s)$ and $Q(s)$, we can get

$$
\begin{cases}
C_1(s)=\dfrac{2\lambda_1 s^{\alpha_1}+1}{2\lambda_2 s^{\alpha_2}+1} \\
C_2(s)=\dfrac{2\lambda_2 T s^{\alpha_2+1}+Ts+2\lambda_2 s^{\alpha_2}+1}{K\lambda_2{}^2 s^{2\alpha_2-1}}=\dfrac{2T}{K\lambda}s^{2-\alpha_2}+\dfrac{T}{K\lambda^2}s^{2-2\alpha_2}+\dfrac{2}{K\lambda}s^{1-\alpha_2}+\dfrac{1}{K\lambda^2}s^{1-2\alpha_2}
\end{cases}
\tag{22}
$$

From eq.(22), the change of the value 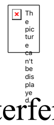 and 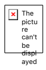 can adjust the tracking performance of the system, and the anti-interference of the system can't be influenced. The change of the value λ_2 and α_2 can adjust the anti-interference performance of the system, while it can have an impact on the tracking performance of the system at the same time. So the value λ_2 and α_2 should be determined according to the anti-interference performance of the system, and then the value 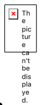 and 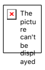 are determined. Finally, the system can obtain good position tracking effect and anti-interference performance at the same time.

In order to verify the validness of the designed controller, simulation is done to track sine curve and step curve by using the two-DOF fractional order internal model controller, the fractional order internal model controller and the two-DOF integer-order internal model controller. The tracking curves are shown in Figure 8 and Figure 9.

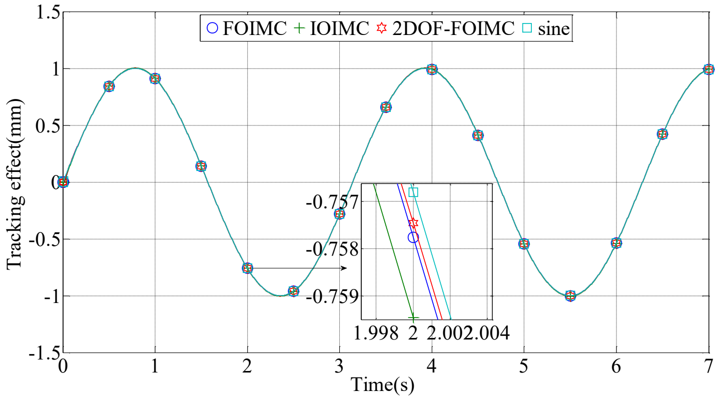

Figure 8. The sine tracking curve under the two-DOF fractional-order internal model controller, the fractional order internal model controller and the integer-order internal model controller

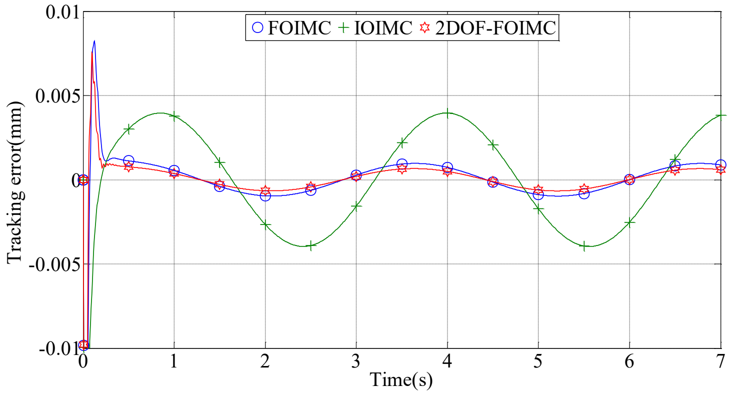

Figure 9. The sine tracking error diagram under the two-DOF fractional-order internal model controller, the fractional order internal model controller and the integer-order internal model controller

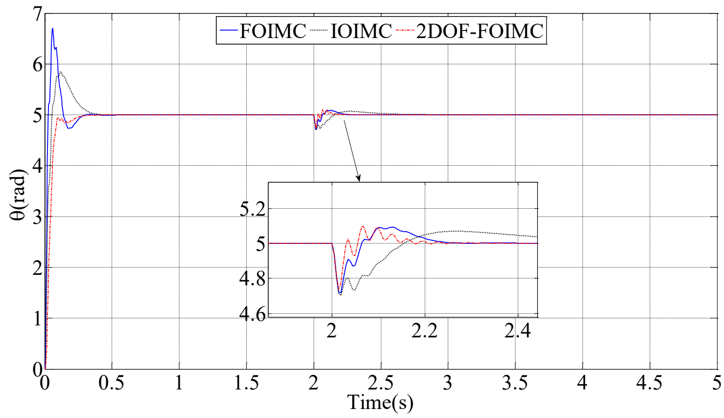

Figure 10. The step tracking curve under the two-DOF fractional order internal model controller, the fractional order internal model controller and the integer-order internal model controller

Table 1. The parameters of permanent magnet synchronous motor

Parameter	Meaning	Value	Unit
K_s	Proportional coefficient of	$5/\pi$	/

	ball screw		
L	Motor armature inductance	0.0027	H
R	Motor armature resistance	1.3	Ω
p_n	Motor pole-pair number	1	/
J	Moment of inertia of motor rotor and screw	0.00188	$Kg{\cdot}m^2$
K_e	Electromagnetic torque coefficient	0.167	/
τ_V	contravariant time constant	0.0001	s
K_n	Inverter control gain	4.43	/

In Figure 8 and Figure 9, the two-DOF fractional order internal model can track the sine curve effectively and there is no overshoot, which demonstrates that the proposed control algorithm can adjust the tracking effect of the system and keep the movement precision of the system. In Figure 10, the position tracking performance of the two-DOF fractional order internal model controller is superior to the fractional order internal model controller, which can make the system free of overshoot and restore to its original state after being disturbed. The parameters are shown in Table 1 and Table 2.

Table 2. The parameters of the controller

Parameter	Meaning	Value	Unit
λ	Fractional order internal model filter parameter	0.012	/
α	Fractional order internal model filter order	1.2	/
λ_I	Integer-order internal model filter parameter	0.05	/

α_1	two-DOF fractional order internal model filter order	0.01	/
λ_1	two-DOF fractional order internal model filter parameter	0	/
α_2	two-DOF fractional order internal model filter order	1.2	/
λ_2	two-DOF fractional order internal model filter parameter	0.01	/

3.2 The redundant force control

Because of the redundant branch, the control of 6PUS-UPU redundant actuation parallel robot becomes very complex. The dynamics model of the redundant branch is related to the force and motion state of the moving platform, which makes the redundant branch very complex and ambiguous. It is difficult to obtain good control effect by using conventional controller.

Torque control is based on current loop control, the redundant branch of AC servo system of the redundant actuation parallel robot uses current loop to control. Considering the stability and simplicity of the system, current loop can be simplified into a first-order inertial link.

$$N(s) = \frac{K}{Ts+1} \tag{23}$$

In Eq.(23), T is the time constant, K is the open-loop gain.

In this paper, according to the requirement of the redundant force branch control of the parallel robot, the fractional order internal model PID controller of the force branch is designed based on the simplified model. According to the design principle of the internal model controller, the fractional order internal model controller is designed as Eq.(24)

$$T(s) = g(s)N^{-1}(s) \tag{24}$$

where $g(s)$ is low-pass filter. The integer order of the low pass filter is extended to the fractional order, then the fractional order filter is as Eq.(25)

$$g(s) = \frac{1}{1+\mu s^{\upsilon}} \tag{25}$$

According to the design principle of the internal model controller, the fractional order internal model controller of the force branch is

$$R(s) = \frac{T}{K\mu}s^{1-\upsilon} + \frac{1}{K\mu}s^{-\upsilon} \tag{26}$$

According to Eq.(26), when the filter order is $v = 1$, $R(s)$is the equivalent of the integer-order PI controller. When the filter order is $0 < v < 1$, $R(s)$ is the equivalent of the fractional order ID controller. When the filter order is $1 < v < 2$, $R(s)$ is the equivalent of the fractional order II controller.

The fractional order internal model force controller can improve the anti-interference capability of the system effectively, but its force tracking performance is not good enough. In order to further improve the tracking performance of the redundant force branch, the fuzzy fractional order internal model control algorithm is proposed based on the fractional order internal model control algorithm.

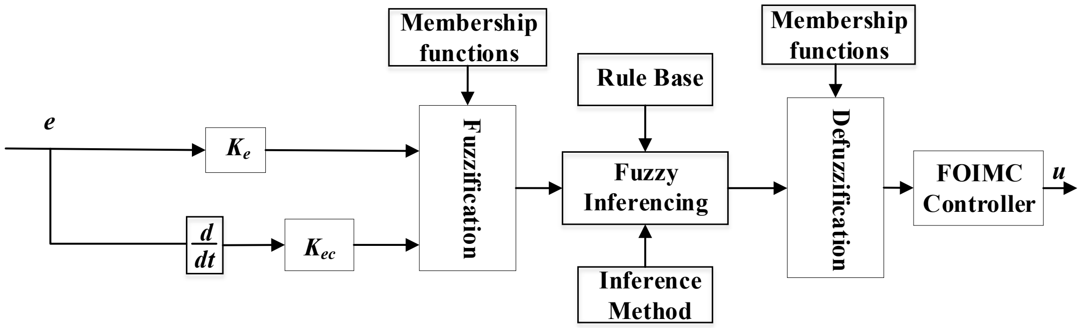

Figure 11. The basic structure of the redundant force branch control

The implementation of the fuzzy controller requires several parts, such as quantization factors, fuzzification, rule base, inference engine and de-fuzzification. Here is a brief introduction to the several parts.

The fuzzy controller needs to normalize the input and the output, and the input variable needs to multiply the quantization factors to realize the transformation between the discrete values and continuous values. In this paper, the range is [-6,6]. The output of the fuzzy controller also requires the scale factor to implement the continuous output of the controller .We assume that the actual range of the input of the fuzzy controller is [-$|e_{max}|$, $|e_{max}|$], [-$|ec_{max}|$, $|ec_{max}|$], the actual range of the output of the fuzzy controller is [-$|u_{max}|$, $|u_{max}|$]. The quantization factors K_e, K_{ec} and the scale factor K_u can be expressed as follows.

$$K_e = 6 / |e_{\max}|,\ K_{ec} = 6 / |ce_{\max}|,\ K_u = 6 / |u_{\max}| \tag{27}$$

After determining the quantization factors K_e, K_{ec} and the scale factor K_u, the fuzzy inputs E and CE can be obtained as follows.

$$\begin{cases} E = \langle K_e \cdot e \rangle \\ EC = \langle K_{ec} \cdot ec \rangle \end{cases} \tag{28}$$

$\langle \cdot \rangle$ means rounding in Eq.(28). Then the actual control output of the fuzzy controller u is expressed as follows.

$$u = \frac{U}{K_u} \tag{29}$$

The input of the fuzzy controller is error and change rate of error, and the output is the output of the controller. They are accurate values, so they need to be mapped to the range of language variables. In this paper, the input language variables are E and EC, and the output language variable is U, and their fuzzy sets are $[NB, NM, NS, ZO, PS, PM, PB]$, representing "negative big value", "negative middle value", "negative small value", "zero", "positive small value", "positive middle value", "positive big value" respectively. The value of the language variable is a fuzzy subset on the domain, which needs to be described by the membership function. If membership functions is selected different, control results are also different.

In the paper, the Gauss membership function is used to describe the fuzzy subset, and is used as the input and output because it has the characteristics of continuous smoothness and having derivative everywhere. The Gauss membership function is:

$$\mu(x) = \exp\left[-(x-c)^2 / 2\sigma^2\right] \tag{30}$$

Where c is the center value of the membership function and σ is the curve width. The Gauss membership function of the input and output is shown in Figure 12.

The rule base is the core of the fuzzy controller, and it mainly depends on the designed experience of experts. Fuzzy rules are as shown in Table 3, using the "IF-THEN" statement and logical AND operation, that is:

IF E is NB AND EC is NB， THEN U is PB.

Table 3. The control rules

U \ *EC* / *E*	NB	NM	NS	ZO	PS	PM	PB
NB	NB	NB	NB	NB	NM	NS	ZO
NM	NB	NB	NM	NM	NS	ZO	ZO
NS	NB	NM	NM	NS	ZO	ZO	PS
ZO	NM	NS	NS	ZO	PS	PS	PM
PS	NS	ZO	ZO	PS	PM	PM	PB
PM	ZO	ZO	ZO	PM	PM	PB	PB
PB	ZO	PS	PS	PB	PB	PB	PB

In the rule base, we use the minimum method to perform logical AND operation. Based on the role of each rule in the rule base, the inference engine gives the inference method of the whole control action. In this paper, we use the Mamdani fuzzy inference algorithm to provide overall control action. The 3D surface diagram between input and output is shown in Figure 13.

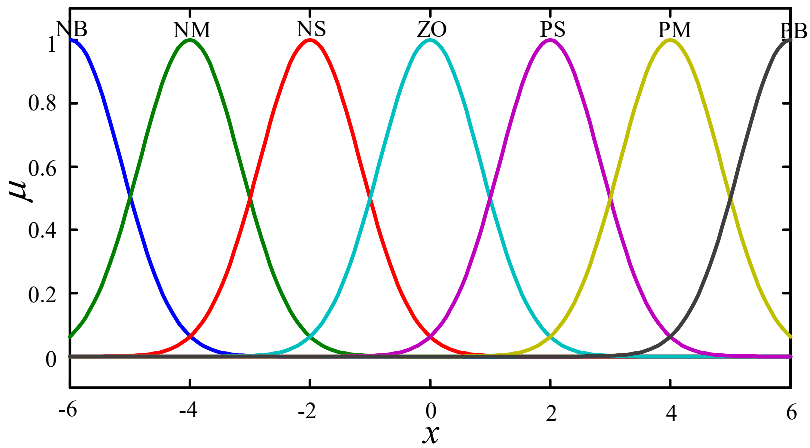

Figure 12. Gauss membership function

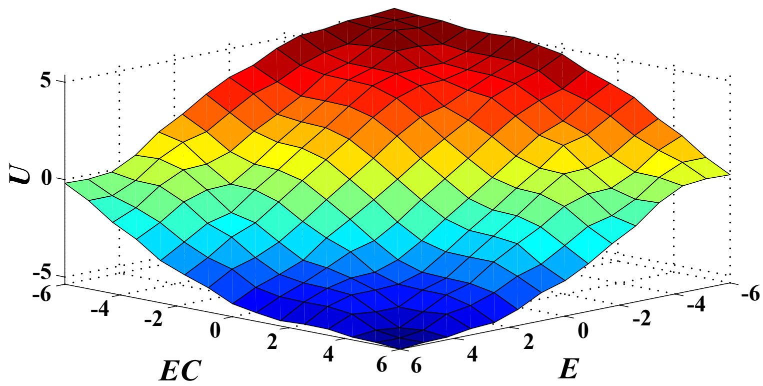

Figure 13. The 3D surface diagram under the fuzzy rules

De-fuzzification is the opposite operation of fuzzy interface. It converts the fuzzy output to continuous and accurate values. The most commonly used de-fuzzification method is the center-of-gravity method, so in this paper, the center-of-gravity method is used as the de-fuzzification method.

4. Matlab/Adams result analysis

We use MATLAB/Simulink and ADAMS joint simulation to testify the control effect of the controller based on the 6PUS-UPU simulation platform. The output of the simulink (the control of the six branches) can be used as the input of the ADAMS, and the output of the ADAMS (the first five branches of the displacement, the sixth branch of the force) can be used as the input of simulink. Fig.14(a) is the whole diagram of MATLAB/ADAMS joint simulation. Fig.14(b) is the virtual model of the 6PUS-UPU redundantly actuated parallel robot in ADAMS. This section will discuss the tracking trajectory obtained from the proposed control algorithm and methods of noise suppression, and plan the moving path of the moving platform. These numbers represent the center coordinates of the moving platform in Figure 15.

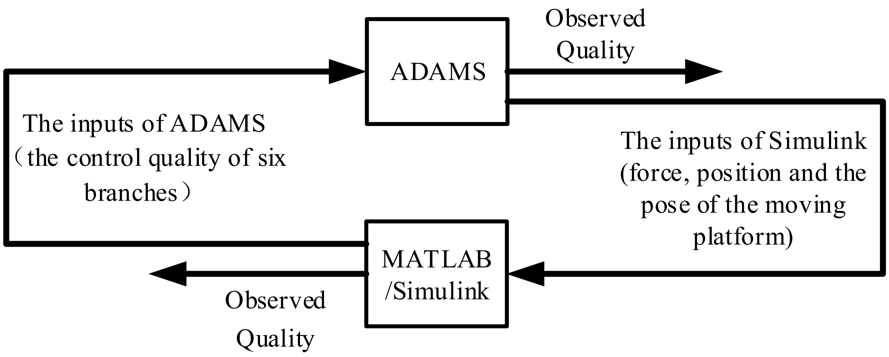

(a) MATLAB/ADAMS joint simulation diagram

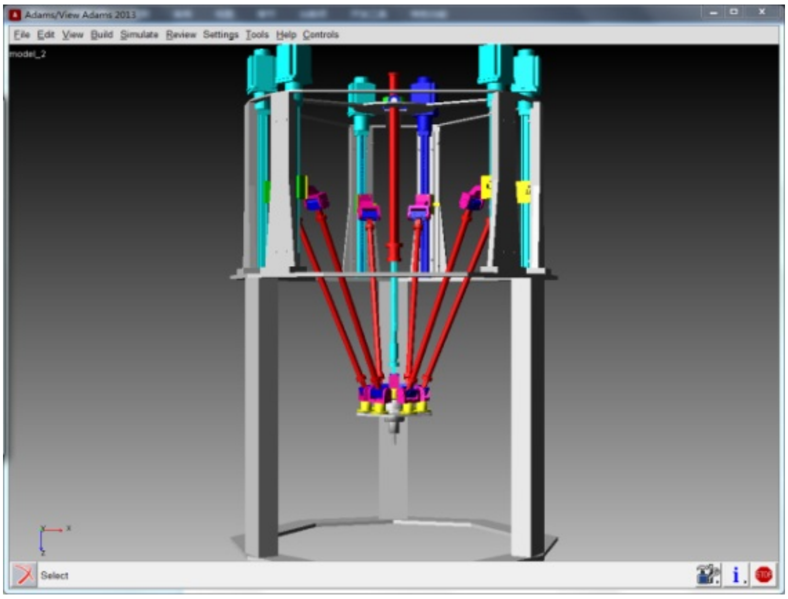

(b) The virtual model of 6PUS-UPU redundantly actuated parallel robot

Figure 14. 6PUS-UPU redundant actuation parallel robot simulation platform

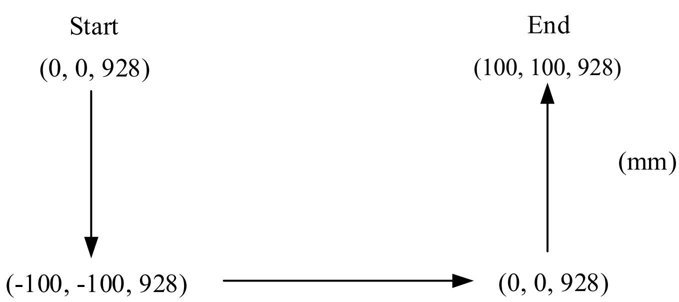

Figure 15. The theoretical planning trajectory of the moving platform

In order to further verify the rationality of the proposed control algorithm, the designed fuzzy fractional-order internal model controller is applied to the redundant branch and then the joint simulation is performed. The first five branches of the mechanism use the two-DOF fractional-order internal model controller. Then the two-DOF fractional order internal model controller is compared with the integer-order internal model controller and the fractional order internal model controller with interference and without interference. Finally, the simulation results are analyzed. The simulation results are shown in Figure 16 to Figure 19.

The theoretical displacement after planning is shown in Figure 16. The smaller the motion error of the system under the path is, the higher the motion precision of the parallel robot is. In Figure 17, when the integer-order internal model controller is used to control the system, the slider displacement error is between -0.4 ~ 0.3mm, so the position error still need to be improved. Figure 18 shows that when the fractional order internal model controller is used to control the system, the slider displacement of the parallel robot reach a smaller range, which is between -0.04 ~ 0.05mm. The proposed fractional order internal model controller can make the parallel robot maintain a lower motion error and improve the motion precision of the system.

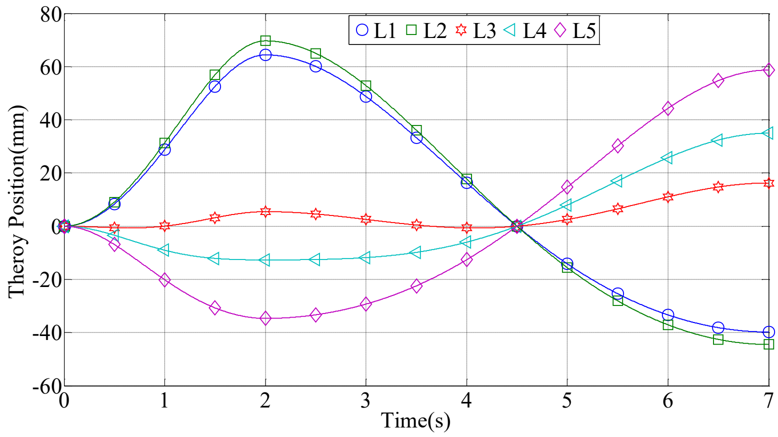

Figure 16. The desired displacement of the first five branches of the parallel robot

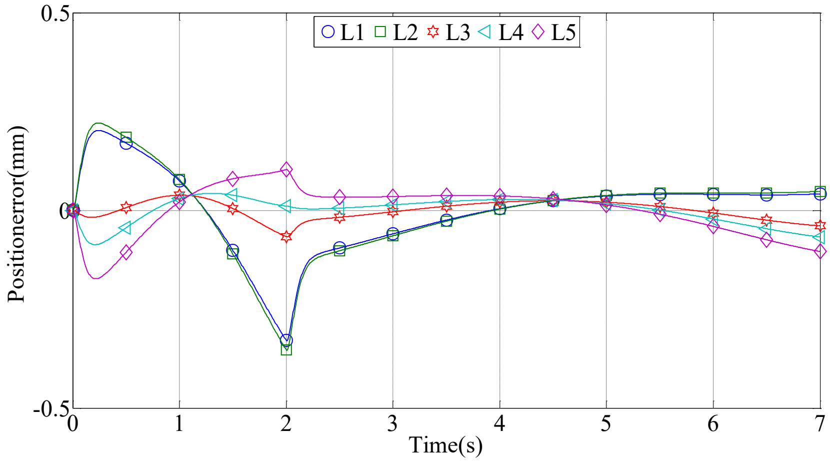

Figure 17. The displacement error of the first five branches controlled the integer-order internal model controller

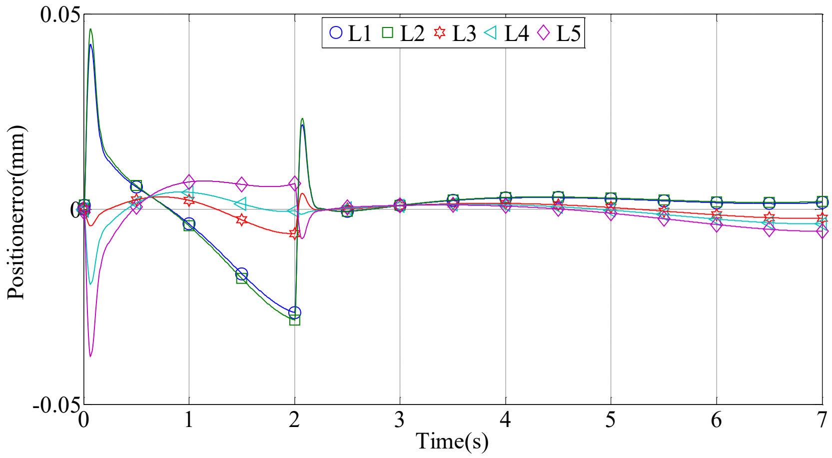

Figure 18. The displacement error of the first five branches controlled the fractional-order internal model controller

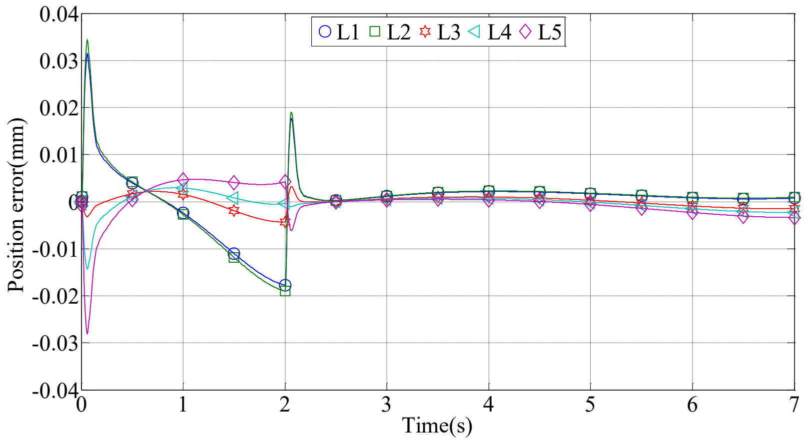

Figure 19. The error diagram of the position branches co-simulated by MATLAB/ADAMS

The error curve of the first five position branches is shown in Figure 19. The two-DOF fractional-order internal model controller makes the system possess a smaller error scope, which is -0.03~0.035mm. And it can independently adjust the anti-interference performance and the dynamic performance, and make the adjustment more convenient.

From Figure 20 to Figure 23, there is good force tracking effect when the fractional order internal model controller and the integer order internal model controller are used as the force controller of the sixth branch. And the internal force error of the system controlled by the fractional order internal model controller is smaller compared with the integer order internal model controller. The fractional order internal model controller can make the system run stably and reduce the probability that the system will damage the machine due to excessive internal force.

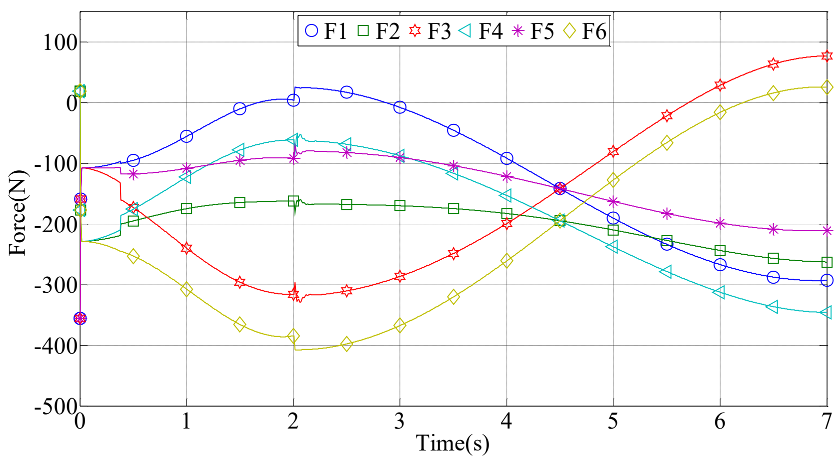

Figure 20. The driving force of each branch controlled by the integer-order internal model controller

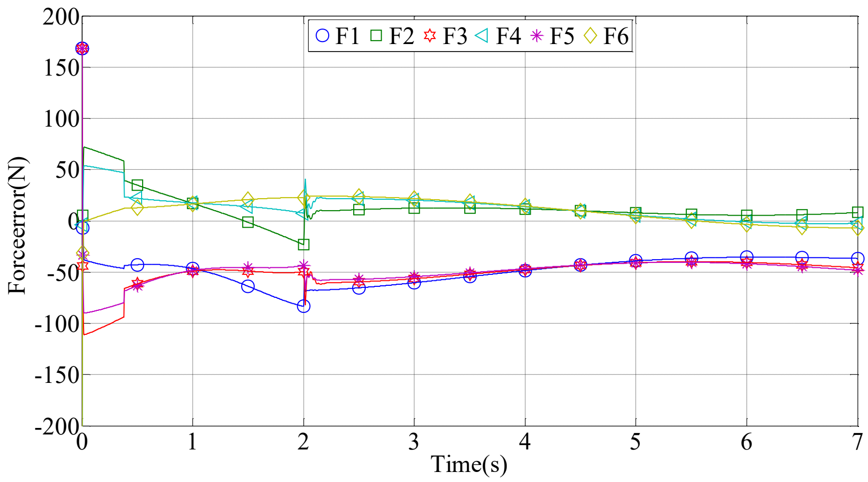

Figure 21. The driving force error of each branch controlled by the integer-order internal model controller

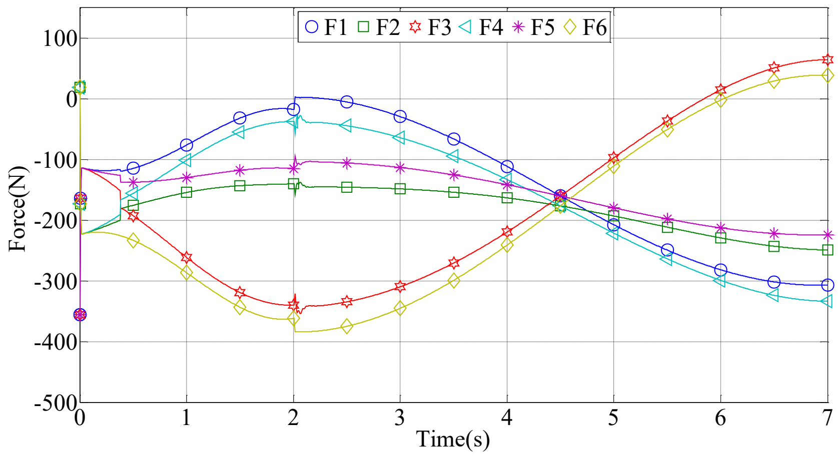

Figure 22. The driving force of each branch controlled by the fractional order internal model controller

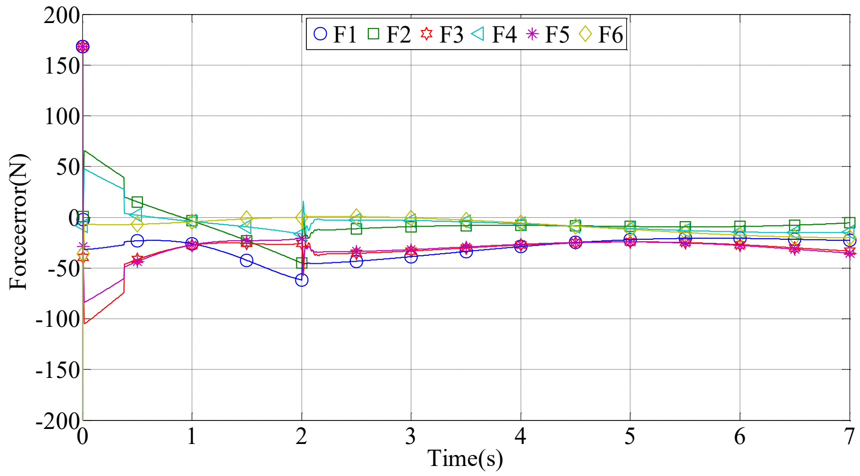

Figure 23. The driving force error of each branch controlled by the fractional order internal model controller

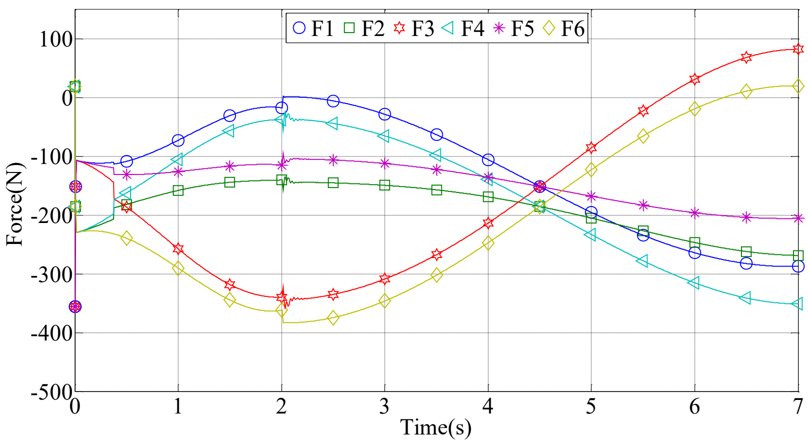

Figure 24. The driving force curve of each branch controlled by the fuzzy fractional order internal model controller without interference

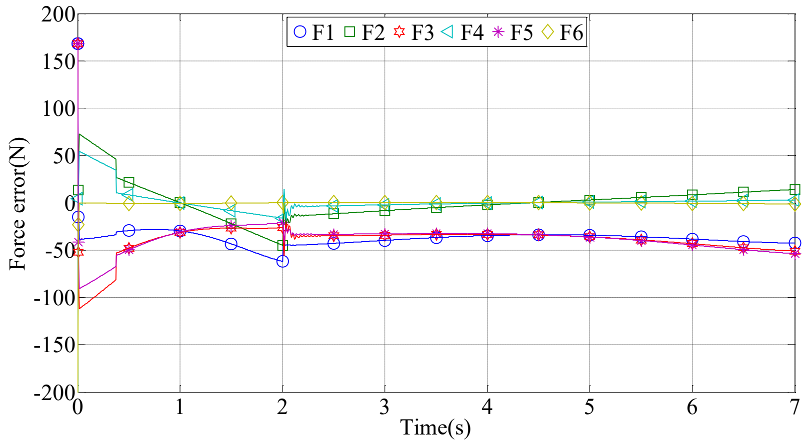

Figure 25. The driving force error of each branch controlled by the fuzzy fractional order internal model controller without interference

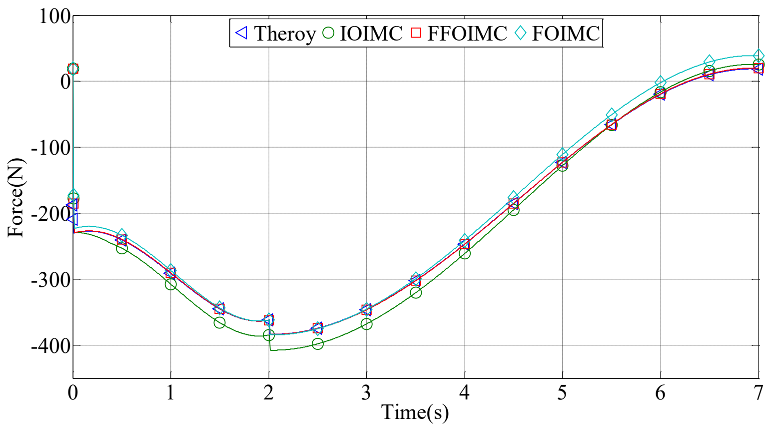

Figure 26. The tracking effect of driving force by using the fuzzy fractional order internal model controller, the fractional order internal model controller and the integer-order internal model controller respectively

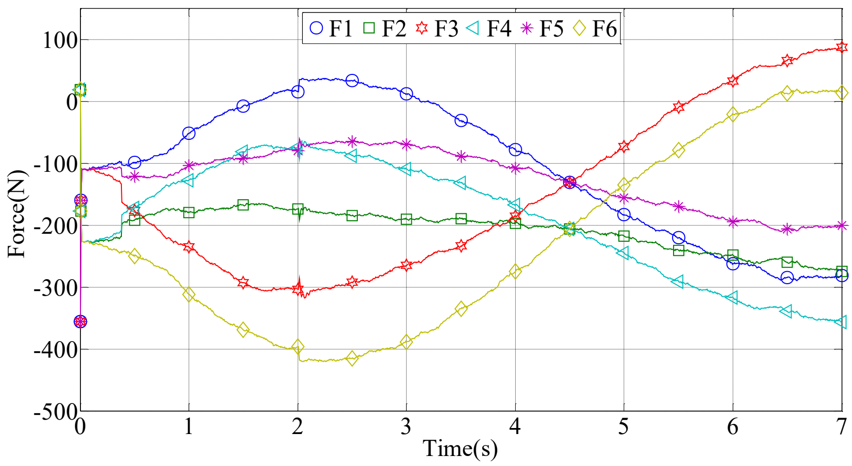

Figure.27. The driving force curve of each branch controlled by the integer-order internal model controller with interference

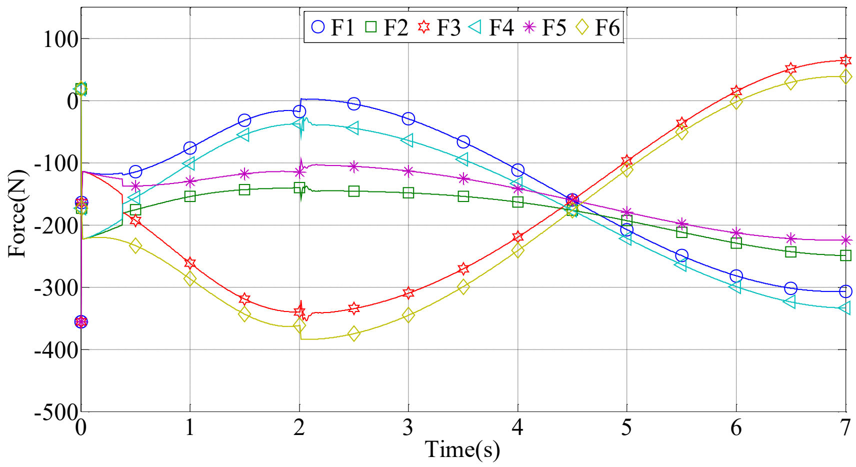

Figure 28. The driving force curve of each branch controlled by the fractional-order internal model controller with interference

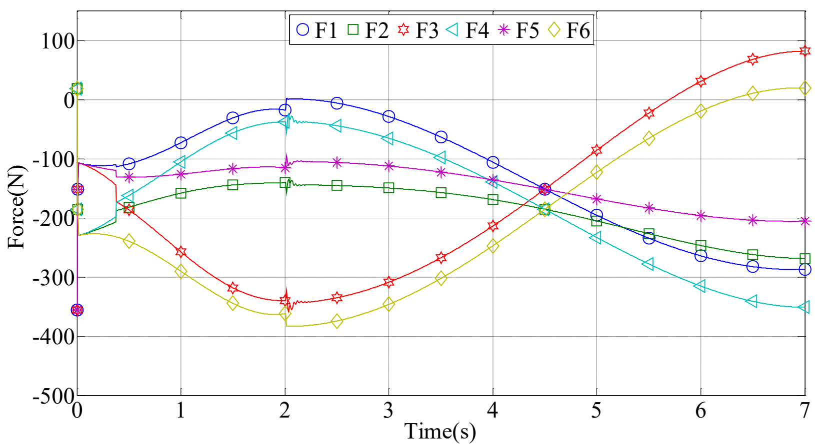

Figure 29. The driving force error of each branch controlled by the fuzzy fractional order internal model controller with interference

From Figure 24 to Figure 26, the force tracking performance is improved obviously after adding the fuzzy theory to the fractional order internal model controller. Moreover, the fuzzy fractional order internal model controller not only has good anti-interference performance like the fractional order internal model controller, but also increases the force tracking ability of the sixth branch and reduces the tracking error because of introducing fuzzy control. Figure 26 shows that the tracking performance of the fuzzy fractional order internal model controller is obviously superior to that of the fractional order internal model controller, that is, the tracking error of the redundant branch is obviously reduced, the internal force of the system can be optimized and the overall control performance of the parallel robot is effectively improved.

In order to further verify the anti-interference ability of the controller for uncertain interference of the whole parallel robot system, in this paper White Gaussian Noise will be added to the sixth branch of the redundantly actuated parallel robot. As shown in Figure 27, Figure 28 and Figure 29, the parallel robot is co-simulated when it is controlled by the integer-order internal model controller the fractional order internal model controller and the fuzzy fractional order internal model controller respectively.

Figure 27 shows that the curve of the driving force controlled by the integer order internal model controller has a certain fluctuation. But overall the controller can suppress the uncertain interference, and meet the anti-interference performance under general conditions. Figure 28 shows that the force curve of the system controlled by the fractional order internal model controller is smooth and has good anti-interference performance, which can maximally keep the system running smoothly under uncertain interference. The fractional order internal model algorithm used in the redundant branch of the parallel robot can not only effectively improve the control precision of the driving force of each branch, but also can improve the robustness of the robot control system, and improve the ability of overcoming the uncertain interference. Figure 29 shows that the system has the same anti-interference performance as the fractional order internal model controller after adding White Gaussian Noise, and the actual driving force curve of each branch is smooth. The result shows that the method can not only improve the control performance of the driving force of the system, but also ensure the system possesses a splendid ability to suppress the uncertain interference.

In order to further quantitatively analyze the superiority of the fuzzy fractional order internal model controller to the fractional order internal model controller and integer-order internal model controller, in this paper the evaluation criterion of average driving force error is established.

$$I_{FF} = \frac{|E_{FFOIMC} - E_{FOIMC}|}{|E_{FOIMC}|}, I_{FFI} = \frac{|E_{FFOIMC} - E_{IOIMC}|}{|E_{IOIMC}|}, I_{FI} = \frac{|E_{FOIMC} - E_{IOIMC}|}{|E_{IOIMC}|}$$

The driving force control precision of each branch is shown in Table 4. In Table 4, E_{FFOIMC}, E_{FOIMC}, E_{IOIMC} represent the average value of the driving force error using the fuzzy fractional-order internal model controller, the average value of the driving force error using the fractional order internal model controller and the average value of the driving force error using the integer-order internal model controller respectively. I_{FF} represents the driving force increment of control precision using the fuzzy fractional order internal model controller compared with the fractional order internal model controller. I_{FFI} represents the driving force increment of control precision using the fuzzy fractional order internal model controller compared with the integer order internal model controller. I_{FI} represents the driving force increment of control precision using the fractional order internal model controller compared with the integer-order internal model controller.

Table 4. The increment of the fuzzy fractional order internal model controller compared with the fractional order internal model controller and the integer-order internal model controller

Branch	$E_{FFOIMC}(N)$	$E_{FOIMC}(N)$	$E_{IOIMC}(N)$	$I_{FF}(\%)$	$I_{FFI}(\%)$	$I_{FI}(\%)$
1	38.13	30.55	49.00	24.81	22.18	37.65
2	12.66	13.53	14.07	6.43	10.02	3.84
3	39.86	32.63	51.53	22.16	22.65	36.67
4	5.37	10.10	14.01	46.83	61.67	27.90
5	38.56	31.20	49.95	23.59	22.80	37.54
6	0.62	8.00	13.07	92.25	95.26	38.79

Table 4 shows that E_{FFOIMC} and E_{FOIMC} of each branch is less than E_{IOIMC} of each branch, which means the performance of the 6PUS-UPU redundant actuation parallel robot with the fuzzy fractional order internal model controller and the fractional order internal model controller is obviously better than with the integer order internal model controller with interference. I_{FF} indicates the force tracking ability of the sixth redundant branch is improved significantly and the tracking error is reduced the force tracking performance is improved obviously after introducing the fuzzy theory to the fractional order internal model controller.

5 Conclusion

The two-DOF fractional order internal model controller is proposed in the position branch of the 6PUS-UPU. This controller has the advantages both of two algorithms. It not only has high tracking performance of the fractional order internal model controller, but also can adjust the tracking performance and anti-interference performance according to requirements. The fractional order internal model controller is incorporating into the fuzzy control algorithm, then the fuzzy fractional order internal model algorithm is proposed. The fuzzy fractional order internal model controller can not only guarantee the driving force control precision of the system, but also has excellent anti-interference performance of the fractional order internal model controller. The Matlab/Adams results show that the proposed algorithms can reduce the dependence of the system on the model, further improve the motion precision of the position branches and the force tracking performance, and optimize the internal force of the system.

6 Acknowledgments

The work was supported by the [National Natural Science Foundation of China] under Grant [number 61773333, 61473248].

References

Krzysztof Tchoń, Joanna Ratajczak, 2016. Dynamically consistent Jacobian inverse for non-holonomic robotic systems. Nonlinear Dynamics. 85(1), 107-122.

Wen H, Xu W, Cong M, 2015. Kinematic Model and Analysis of an Actuation Redundant Parallel Robot With Higher Kinematic Pairs for Jaw Movement[J]. IEEE Transactions on Industrial Electronics, 62(3), 1590-1598.

Sébastien B., François C., Philippe M., 2017. Revisiting the Determination of the Singularity Cases in the Visual Servoing of Image Points Through the Concept of Hidden Robot[J], IEEE Transactions on Robotics, 33(3), 536-546.

Pham Q C, Stasse O,2015. Time-Optimal Path Parameterization for Redundantly Actuated Robots: A Numerical Integration Approach[J]. IEEE/ASME Transactions on Mechatronics, 20(6), 3257-3263.

Taghirad H D, Bedoustani Y B, 2011. An Analytic-Iterative Redundancy Resolution Scheme for Cable-Driven Redundant Parallel Manipulators[J]. IEEE Transactions on Robotics, 27(6), 1137-1143.

Savran A I, Beke A, Kumbasar T, et al, 2015. An IMC based Fuzzy Self-Tuning Mechanism for Fuzzy PID Controllers[C]//International Symposium on Innovations in Intelligent Systems and Applications, Madrid, Spain. IEEE, September,1-7.

Wang Z, Duan R, Sun G, et al, 2016. Hydraulic Quadruped Robot Joint Force Control Based on Double Internal Model Controller[J]. International Journal of Control and Automation, 9(1), 241-250.

Kostić M D, Mataušek M R, Popović D, 2016. Modified Internal Model Control For A Therapeutic Robot[J]. Facta Universitatis, Series: Electronics and Energetics, 30(1), 137-144 (2016)

Hou Y, Tong S, 2016. Adaptive fuzzy backstepping control for a class of MIMO switched nonlinear systems with unknown control directions[J]. Complexity, 21(6), 155-166.

Pagavathigounder B, Dhanasekaran N, Liyakath Ali J B, 2016. Robust guaranteed cost control for discrete-time systems via partially delay-dependent controller with linear fractional uncertainties[J]. Complexity, 21(S2), 113-122.

Sondhi S, Hote Y V, 2014. Fractional IMC Design for Fractional Order Gas Turbine Model[C]//International Conference on Industrial and Information Systems, Gwalior, India IEEE, 1-5.

Li D, Fan W, Jin Q, et al, 2010. An IMC-PI~λ D~μ Controller Design for Fractional Calculus System[C]// Chinese Control Conference, 3581-3585.

Maâmar B, Rachid M, 2014. IMC-PID-fractional-order-filter controllers design for integer order systems[J]. Isa Transactions, 53(5), 1620-1628.

Zhu Q, Yin Z, Zhang Y, et al, 2016. Research on Two-Degree-of-Freedom Internal Model Control Strategy for Induction Motor Based on Immune Algorithm[J]. IEEE Transactions on Industrial Electronics, 63(3), 1981–1992.

Liu X, Wang X, Zheng K, et al, 2014. Design of variable pitch-control system based on two-degree-of-freedom internal model control[C]// International Conference on Information Science, Electronics and Electrical Engineering. IEEE, 1348-1352.

Vinopraba T, Sivakumaran N, Narayanan S, 2011. IMC based Fractional order PID controller[C]// IEEE International Conference on Industrial Technology. IEEE, 71-76.

Lakshmana G N V, Jeevaraj S, Geetha S, 2016. Total ordering for intuitionistic fuzzy numbers[J]. Complexity, 21(S2), 54-66.

Zhong Z, Shao Z, Chen T, 2016. Decentralized Piecewise Fuzzy H∞ Output Feedback Control for Large-Scale Nonlinear Systems with Time-Varying Delay[J]. Complexity, 21(S2), 268-288.

Reham, H, F. Bendary, and K. Elserafi, 2016. Trajectory Tracking Control for Robot Manipulator using Fractional Order-Fuzzy-PID Controller. International Journal of Computer Applications, 134(15), 1–8.

Delavari H, Ghaderi R, Ranjbar A, et al, 2010. Fuzzy fractional order sliding mode controller for nonlinear systems[J]. Communications in Nonlinear Science & Numerical Simulation, 15(4), 963-978.

Wang B, Xue J, Wu F, et al, 2016. Stabilization conditions for fuzzy control of uncertain fractional order non-linear systems with random disturbances[J]. IET Control Theory & Applications, 10(6), 637-647.

Wen S, Yu H, Zhang B, et al, 2017. Fuzzy Identification and Delay Compensation based on the Force/Position Control Scheme of the 5-DOF Redundantly Actuated Parallel Robot[J]. International Journal of Fuzzy Systems, 19(1), 124-140.

Wen S, Qin G, Zhang B, et al, 2016. The study of model predictive control algorithm based on the force/position control scheme of the 5-DOF redundant actuation parallel robot[J]. Robotics &

Autonomous Systems, 79(C), 12-25.

Notes on contributors

Shuhuan Wen was born in Heilongjiang, China, on July 16, 1972. She received the PhD degree in control theory and control engineering from the Yanshan University, Qinhuangdao, China in 2005.

She is currently a Professor of automatic control in the Department of Electric Engineering, Yanshan University. She has coauthored one book, about 40 papers. Her research interests include humanoid robot control, force/motion control of parallel robot, Fuzzy control, 3-D object recognization and reconstruction.

Dr. Wen was a Visiting Scholar of the Ottawa University, Carleton University and Simon Fraser University in Canada from 2011 to 2013.

Di Zhang was born in HeBei, China, in May, 1995. She received the Bachelor degree in the Department of Electrical Engineering, North China University of Science and Technology in 2017.

She has coauthored one journal paper. Her research interests are on humanoid robot control and multi-robot cooperation.

Baowei Zhang was born in HeBei, China, in May, 1989. He received the Bachelor degree in the Department of Electric Engineering, Chengdu University in 2014.

He has coauthored about one journal papers. His research interests are focused on Multi degree of freedom parallel robot control.

H.K. Lam received the B.Eng. (Hons.) and Ph.D. degrees from the Department of Electronic and Information Engineering, The Hong Kong Polytechnic University, Hong Kong, in 1995 and 2000, respectively. During the period of 2000 and 2005, he worked with the Department of Electronic and Information Engineering at The Hong Kong Polytechnic University as Post-Doctoral Fellow and Research Fellow respectively. He joined as a Lecturer at King's College London in 2005 and currently is a Reader.

His current research interests include intelligent control and computational intelligence. He has served as a program committee member and international advisory board member for various international conferences and a reviewer for various books, international journals and international conferences. He is an associate editor for IEEE Transactions on Fuzzy Systems, IET Control

Theory and Applications, International Journal of Fuzzy Systems and Neorocomputing; and guest editor for a number of international journals. He is in the editorial board of Journal of Intelligent Learning Systems and Applications, Journal of Applied Mathematics, Mathematical Problems in Engineering, Modelling and Simulation in Engineering, Annual Review of Chaos Theory, Bifurcations and Dynamical Systems and The Open Cybernetics and Systemics Journal. He is an IEEE senior member.

He is the coeditor for two edited volumes: Control of Chaotic Nonlinear Circuits (World Scientific, 2009) and Computational Intelligence and Its Applications (World Scientific, 2012), and the coauthor of the monograph: Stability Analysis of Fuzzy-Model-Based Control Systems (Springer, 2011).

Hongbin Wang Professor in the College of Electrical Engineering, Yanshan University. He received his Ph.D. degree in control theory and control engineering from Yanshan University in 2005. His research interest covers process automation, robot control technology, variable structure control, robust control, and visual servo.

Yongsheng Zhao received his bachelor's degree and the master's degree in mechanical engineering from North-east Heavy Machinery Institute, Qiqihaer, Heilongjiang Province, China in 1983 and 1987, respectively. He re-ceived the Ph.D. degree in mechanical engineering from Yanshan University, Qinhuangdao, Hebei Province, China in 1999. He is currently a professor in Robotics Research Center at Yanshan University. He is currently the vice-chancellor of Yanshan University. His research interests include parallel robot, force sensor, numerical control technique, Fuzzy control, etc. He has coauthored one book, more than 80 papers.